

Deformation studies in the Gulf of Patras, Western Greece

*K. Papazissi, D. Anastasiou, A. Marinou, C. Mitsakaki,
X. Papanikolaou, D. Paradissis*

School of Rural & Surveying Eng., National Technical University of Athens, Greece

Abstract

In the present paper, statistically acceptable strain parameters for a deformation model are evaluated, using GPS data from a geodetic network established in the broader area of the gulf of Patras. Velocities were estimated for the network sites using mainly data from three campaigns, taking place between 1998 and 2000, as well as all previous GPS positions available for the region. The derived velocity field is in congruence with previous works. In order to investigate the tectonic behavior of the area, several models for the secular deformation were applied and the strain tensors for each case were computed and discussed.

1. Introduction

The gulf of Patras is part of the Ionian Islands region which is a unique one in that it behaves as a multiple junction, where all four types of plate boundary (collision, subduction, transform and spreading) occur (Sachpazi et al. (2000)). The gulf lies at the western end of a system of graben structures, among them the Corinth and Rio rifts, associated with the active subduction in the Western Hellenic arc. The outer part of the gulf is a linear trough with a length of ~ 22 km and extensive active faulting of WNW-ESE trend on the southern flank of the trough (Ferentinos et al. (1985)).

Earthquake epicenters in central Greece define a 200 km long and 40 km wide belt from the Aegean to the Ionian Sea with the central part occupied by the Corinth-Patras rift (Doutsos et al. (1992)). The intersection of the Corinth and Rio grabens is delineated by clustering of seismicity, while very low numbers of earthquakes appear in the Patras gulf (Figure 1). A similar picture emerges in the case of the historic earthquakes (550BC-1986AC) for the region (Figure 2). Seismicity records and geotectonic information for the active structures in NW Peloponnese indicate that faults, although relatively small, may generate earthquakes with $5.0 < M_S < 5.8$. Thus, the more recent large earthquakes that occurred in the vicinity attracted attention and were duly investigated (Roumelioti et al. (2004); Ganas et al. (2009)).

Furthermore, the kinematic field of the western part of the Hellenic arc attracted

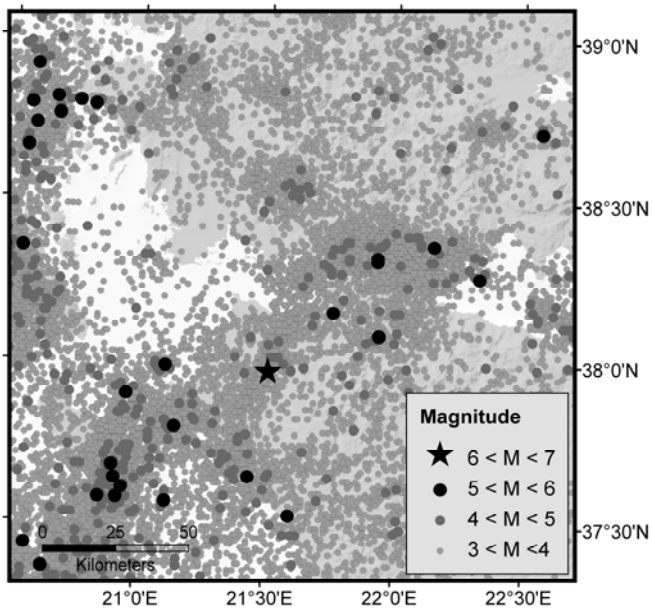


Figure 1: Seismicity map of the region (1980 – 2010).
Data from the database of the National Observatory of Athens

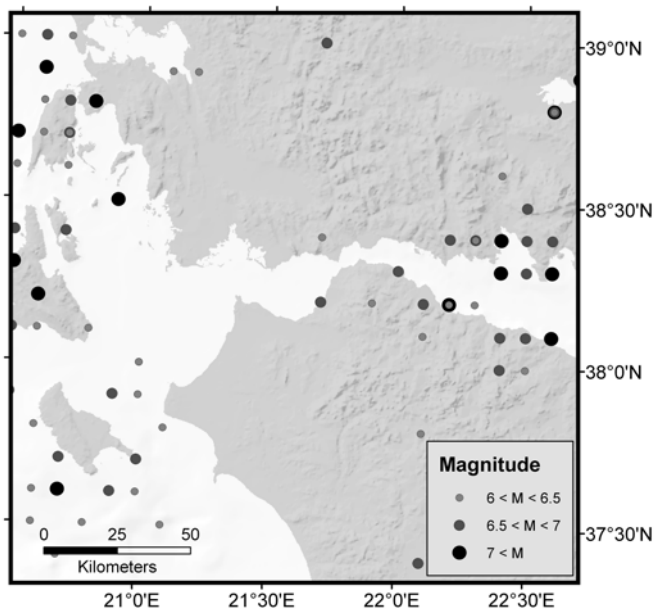


Figure 2. Historical earthquakes for the region with magnitudes $M_s > 6$.
Data from Παπαζάχος Β. και Παπαζάχου Κ., (2003) (in Greek)

attention from the geodetic community since the late eighties. Several GPS campaigns were carried out and the acquisition of the high quality satellite data contributed significantly to the description of the kinematics of the area (Kahle et al. (1995); Muller M. (1995); Hollenstein C. (2006)).

Equivalent attention has been focused on the Corinth gulf which has been extensively investigated, by seismic, geotectonic and geodetic studies for more than twenty years (Briole et al. (2002); Avallone et al. (2004); Bernard et al. (2006)). However, so far, no systematic geodetic work has been carried out on the area surrounding the Patras gulf. The present work is a first attempt to use all available GPS data, compiled from campaigns where the NTUA was involved, to describe the surface deformation pattern.

2. Analysis of GPS data

The GPS geodetic network consists of 31 sites occupied in 3 epochs, namely 1998.79, 1999.42, 2000.51. Most of the points are pillars of the National Geodetic Network, while the rest are markers, established during the various interdisciplinary projects of the past, carried out by both the NTUA and Institutes from abroad. For the majority of pillars a special device was developed for the elimination of centering errors.

Not all of the points were observed in all periods. Figure 3 shows the distribution of the GPS network, as well as the number of epochs each point was occupied. An overview of all relevant information about the GPS network is given in Table 1.

Table 1: Overview of the GPS network

Network details	Epochs	1998.79	1999.79	2000.51
	Days of observations		6	2
Number of points		31	13	28
DREP and DION sessions (in hours)		24	12	24
Points with more than 4 hours sessions		6	1	3
Points with 4 hours sessions		23	10	23

All data processing was carried out with the Bernese V5 software package, using IGS precise orbits, IGS products for the earth rotation (IGS earth rotation parameters), relative receiver antenna Phase Center Variation (PCV) along with the respective satellite phase pattern file and CODE-produced Code Differential Bias (DCB) corrections.

Local ionospheric models for baselines longer than 600 Km were calculated, as well as local tropospheric models for the whole of the network. A single zenith

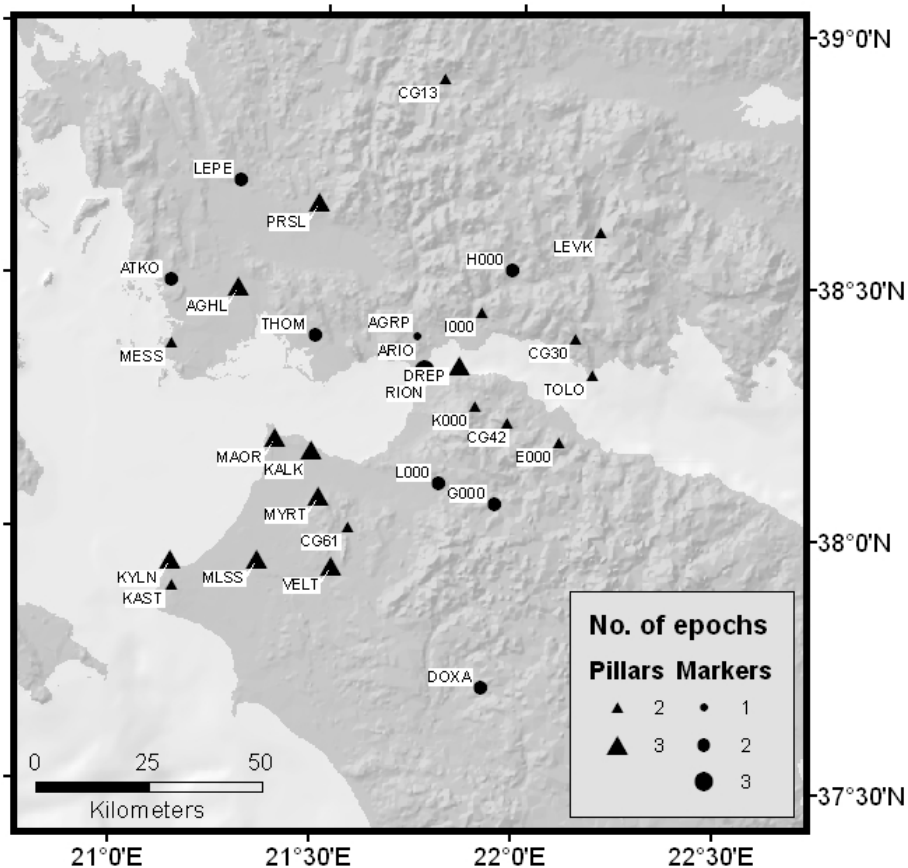


Figure 3. Distribution of the GPS sites and respective epochs of occupation

path delay parameter was estimated every 2 hours per site for the tropospheric models. Automated cycle slip fixing was applied. The Quasi Ionosphere Free Strategy was used for the ambiguity resolution. A relatively low percentage (65%) of ambiguities resolved was accepted, due to the fact that the campaigns took place more than a decade ago and the duration of the observations was a short one in all cases.

Next, all the baseline daily solutions were stacked, to produce final coordinate estimates. For each epoch, the IGS station coordinates were kept stable providing a realization of the ITRF2005 reference frame.

For all epochs, twelve IGS stations were chosen for the realization of the Reference Frame ITRF2005 together with two Hellenic stations; station Drepano (DREP) and station Dionysos (DION). IGS stations were chosen in order to fulfil as closely as possible the criterion of best network geometry, despite the fact that

very few stations were available in the south. The two Hellenic sites were selected because they have the longest sessions of observations; besides Dionysos is one of the oldest sites in Greece, with well estimated tectonic motion. All available baselines between the two Hellenic sites and the twelve IGS stations were used for the realization of the ITRF2005 (Figure 4).

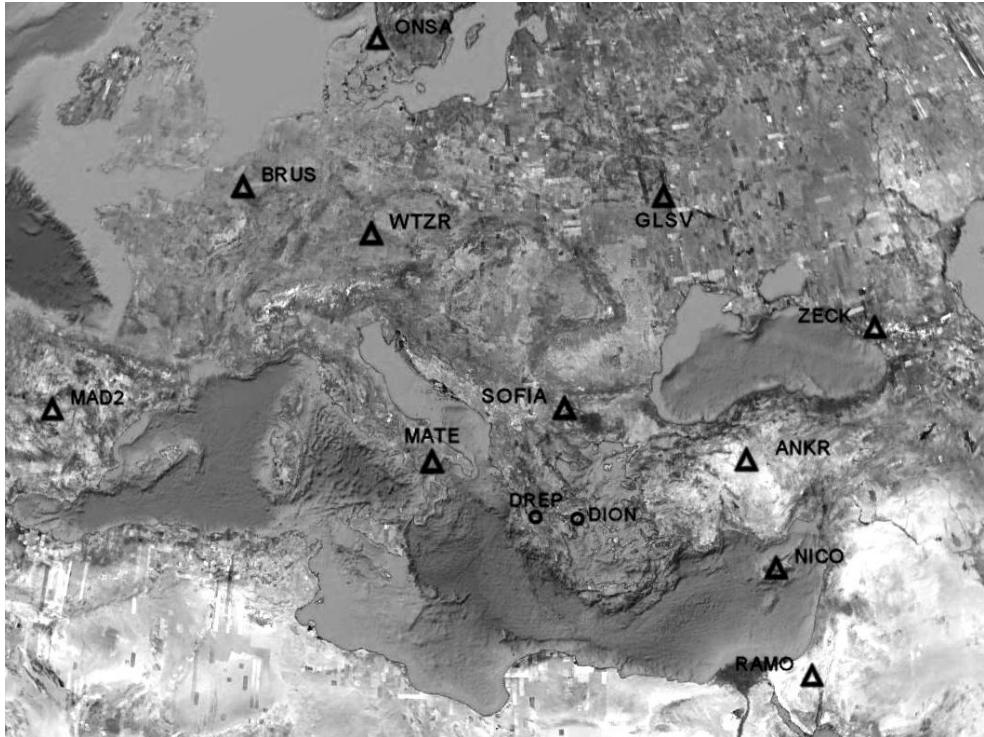


Figure 4: The twelve IGS Stations and the two Hellenic ones used for the realization of the ITRF2005.

All the relevant information regarding the number of points occupied during each campaign, the duration of field observations, the length of sessions etc are presented in Table 1. In all cases, the local network points were connected to the local main station DREP. However, in order to maintain the length of the baselines relatively short, other than the DREP points were used (Table 1, fourth row). In Figures 5, 6 and 7 all the baselines formed for each day and each campaign respectively are presented.

In all cases, more than 70% of the ambiguities were resolved for the local network. However, due to a large amount of cycle slips some points failed to be resolved; for the first campaign point PRSL, RION for the second one and MYRT for the last one.

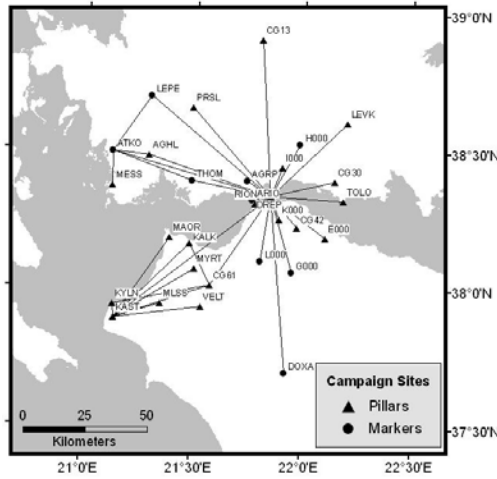


Figure 5: The network for epoch 1998.79

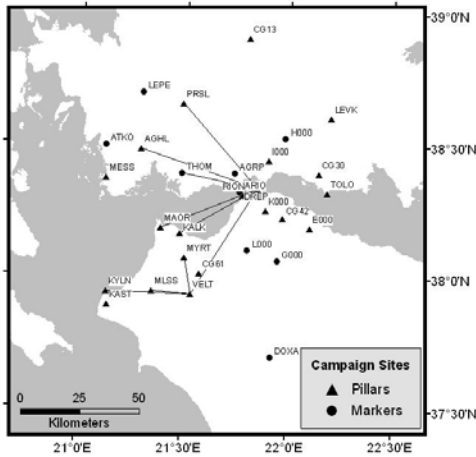


Figure 6: The network for epoch 1999.79

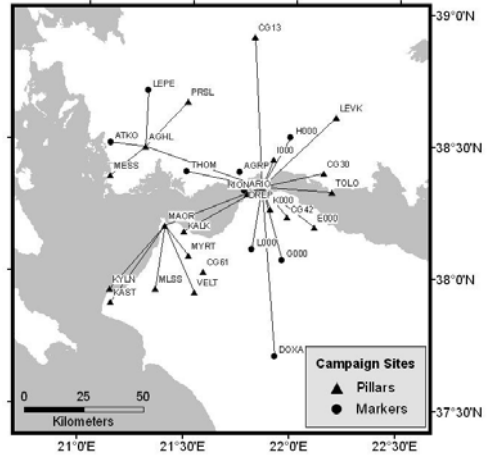


Figure 7: The network for epoch 2000.51

3. The velocity field

The Patras network has been observed piecewise, during the various research projects carried out by the NTUA and the collaborating international institutions, since the nineties. A data base had to be build in order to include all relevant information (initial data and metadata) from all the campaigns.

In order to evaluate velocities for the network points all previous information available in the database was exploited. All solutions were transformed to the common reference frame of ITRF2005 using the official Helmert transformation

parameters (available at http://itrf.ensg.ign.fr/trans_para.php). The kinematic model of Argus and Helfin (1998) was used for the velocity of the European plate with respect to the world, with rates of $V_{north} = +11.4$ mm/yr and $V_{east} = +23.6$ mm/yr.

For each point, the respective time series were used, in order to calculate the velocity vector. In most cases a statistically reliable solution was achieved while, whenever this was not possible, the point was excluded; this was the case for three points. In Table 2 estimated velocities with respect to a stable Europe model as well as their standard deviations are presented.

Table 2: *Velocities with Respect to a stable Europe*

CODE	V_n	σ_{V_n}	V_e	σ_{V_e}	CODE	V_n	σ_{V_n}	V_e	σ_{V_e}
AGHL	-13.6	± 2.0	-7.4	± 6.4	K000	-22.0	± 2.4	-14.7	± 1.4
AGRP	-9.8	± 2.9	-9.1	± 0.5	KAST	-20.5	± 1.2	-16.5	± 2.0
ARIO	-10.0	± 6.1	-14.0	± 1.3	KYLN	-6.7	± 1.3	-11.0	± 3.8
ATKO	-15.9	± 1.3	-5.8	± 1.3	L000	-24.6	± 1.6	-14.2	± 1.2
CG13	-8.7	± 0.8	-5.8	± 1.8	LEPE	-5.4	± 0.6	-8.2	± 0.2
CG30	-1.3	± 0.3	-12.8	± 2.2	LEVK	-5.7	± 0.4	-9.9	± 1.0
CG42	-25.2	± 1.1	-12.7	± 2.1	MAOR	-22.4	± 2.1	-22.0	± 7.2
CG61	-22.8	± 1.1	-14.9	± 1.9	MESS	-6.2	± 1.9	-7.5	± 1.5
DOXA	-24.3	± 0.5	-17.8	± 1.5	MLSS	-21.5	± 0.0	-21.2	± 0.0
DREP	-15.7	± 0.8	-10.9	± 1.1	RION	-11.0	± 0.0	-20.7	± 0.0
E000	-27.5	± 2.4	-14.4	± 1.2	TOLO	-8.7	± 1.2	-17.2	± 2.1
G000	-23.8	± 1.1	-17.9	± 0.7	VELT	-22.0	± 0.4	-21.1	± 1.4
H000	-9.7	± 0.4	-11.4	± 0.7	PRSL	-8.4	± 0.0	-4.4	± 0.0
I000	-9.8	± 1.3	-12.6	± 0.8					

It should be mention here that the average velocity for the Dionysos site estimated from the three campaigns ($V_n = -11.5$, $V_e = 7.6$ mm/yr) is in good agreement with the value ($V_n = -12.9$, $V_e = 8.6$ mm/yr) resulting from several years of observations.

In Figure 8 velocities and corresponding error ellipses referred to a stable Europe are presented. The velocity field has a prominent south west direction while the vectors appear to increase in size from North to South and to slightly rotate towards west. This picture is compatible with the velocity field of Hollenstein et al. (2008), Anastasiou et al. (2009) and Briole et al. (2002), Avallone et al. (2004).

The present work is based on a two-dimensional linear deformation model, while the area under consideration is assumed as a thin calotte on a spherical earth homogeneously deforming. Since the region under study is a limited one distortion due to omitting the curvature would not exceed 10^{-3} in scale and can be ignored.

Besides, because of the average size of displacements, the infinitesimal elastic strain theory is followed without loss of the required precision (Veis et al, (1992); Agatza-Balodimou et al, (1994)). Thus, the parameters of strain inside each deforming block are estimated by least squares.

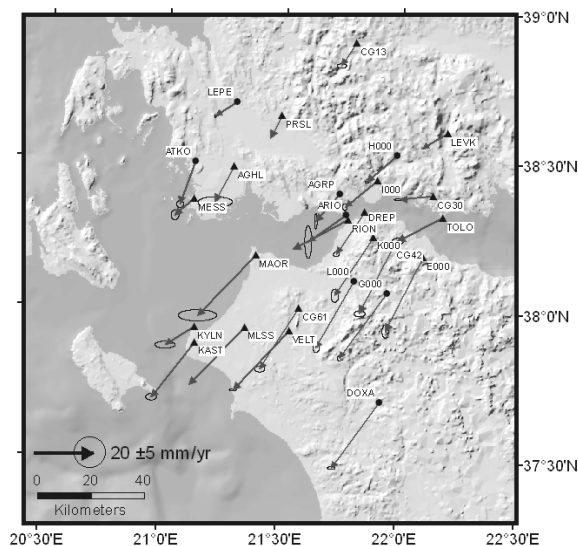


Figure 8: Velocity field respect to stable Europe and corresponding error ellipses

The strain parameters for all cases examined are presented in Table 3.

Table 3: Strain tensor parameters for all cases

Secular motion model		<i>K</i> _{max} (ppm)	<i>K</i> _{min} (ppm)	γ (μ strain/Myrs)	<i>A</i> _z (deg)
single block		+0.178	-0.052	+0.230	12.74
North - south blocks	North	+0.068	-0.115	+0.183	31.08
	South	+0.131	-0.003	+0.135	156.18
East - west blocks	East	+0.230	-0.057	+0.287	19.59
	West	+0.130	-0.133	+0.263	175.72
Four quadrants model	North - East	+0.156	-0.146	+0.302	39.19
	North - West	+0.354	-0.023	+0.330	138.29
	South - East	+0.115	-0.098	+0.213	151.31
	South - West	+0.106	-0.234	+0.340	140.62

In order to get a detailed and realistic pattern for the tectonic behaviour of the Patras gulf, several cases were considered. In the first one the whole area was treated as a single block (Figure 9a). In all other cases the area was assumed as

consisting of blocks with distinct sets of parameters. Thus, in the second case a two blocks with North - South division was considered (Figure 9b). A third case was to divide the area in two blocks (East-West) (Figure 9c). Finally a four blocks model for the region was considered (Figure 9d).

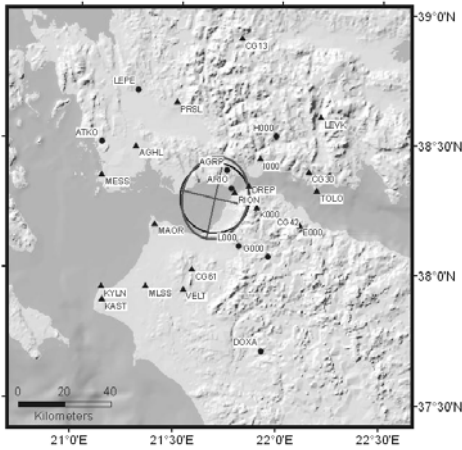


Figure 9a: Strain Tensor for the whole region

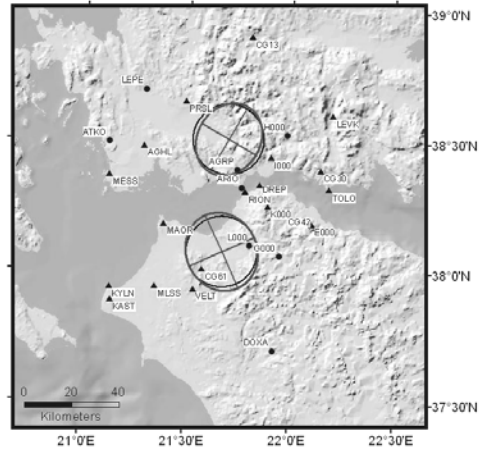


Figure 9b: Two blocks (North-South)

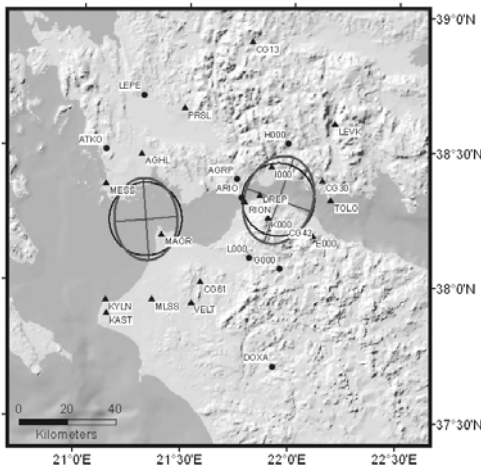


Figure 9c. Two blocks (East-West)

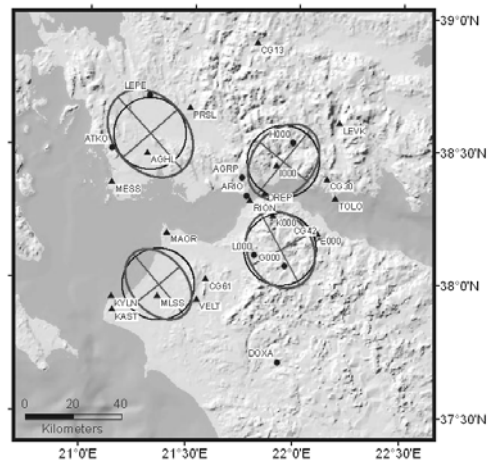


Figure 9d. Four block model

4. Discussion - Conclusions

As mentioned before the velocity field of the gulf of Patras (Figure 8) is in good agreement with previous works. More particularly, it should be mentioned that the velocity field of North Peloponnesus is, quite comparable with Briole et al. (2002)

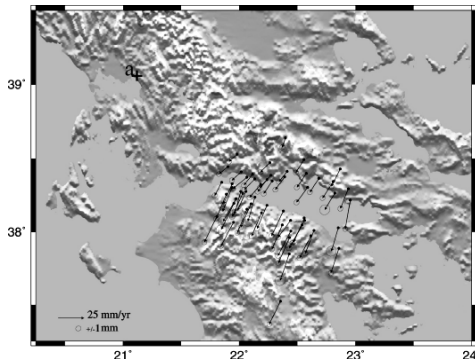


Figure 10: From Briole et al. (2002)

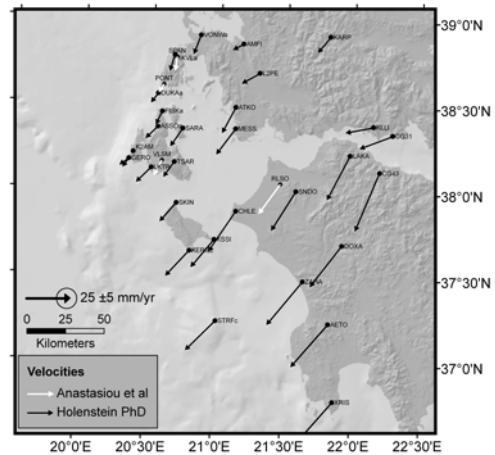


Figure 11: Composite from Hollenstein C. (2006) and Anastasiou et al. (2009)

(Figure 10) and Avallone et al. (2004). On the other hand a more pronounced westward motion of some vectors on the South Sterea Hellas area is in better agreement with Hollenstein C. (2006), Hollenstein et al. (2008) and Anastasiou et al. (2009) (Figure 11).

In the case of the strain analysis an extension with a NNE-SSW direction is apparent when the area has been considered as one block. However, the velocity field of the Patras gulf appears to increase in size gradually from North to South (Figure 8) and this may be interpreted wrongly as an extension, if the area is represented by a single block.

Thus, a second reasonable model to consider was to break the region in two blocks, namely the north and the south one. In this case the north part appears to retain the extensional trend with a slight clockwise rotation of the azimuth of the elongation axis. On the other hand, the south part of the gulf is extending with a NNW-SSE direction.

In the case of the third model a difference in the direction of the deformation can be observed from west to east (Figure 9c). The west part is extending to a NNW direction while the east part is extending to a NNE direction. Compression rates are larger in the west part while extension rates are larger on the east part.

Since the two block models of north-south and east-west indicate a different tectonic behaviour and the seismicity map (Figure 1) signifies a seismically active zone in the south-western part of the gulf of Patras, where the Mihoi June 08, 2008 earthquake of $M_w \sim 6.4$ occurred (Ganas et al. (2009)), a four block model (four quadrants) was also considered (Figure 9d).

The two quadrants of north Peloponnese (south blocks) have similar orientations of the elongation axes, while the strain elements' values are different (Table

3). In the case of south Sterea Hellas (north blocks), the strain tensor of the north-eastern quadrant is comparable to the north one of the two-block model. The behaviour of the northwestern quadrant appears to be in agreement with the general trend of north Peloponnesus. However, it should be mentioned here, that the existence of the westward trend of the velocity field of Sterea Hellas needs further investigation, since the number of sites used is a rather limited one.

Other cases were also examined, such as the division of the region into various blocks, but with no significant improvement in the description of the tectonic behaviour of the area.

As a general remark, the strain accumulation, which appears in some of the models considered, is not so far adequately documented from the available geodetic data.

The geodetic methods work efficiently for monitoring crustal movements if the GPS sites are homogeneously distributed across the major geological features (faults, etc) and a good spatial and temporal coverage for the broader area is ensured. Therefore, for a better understanding of the behaviour of the area, existing points should be reoccupied, since a limited number of epochs are so far available, while the densification of the network should also be considered.

Acknowledgments

The authors would like to thank all the colleagues, national and from abroad, who participated in the interdisciplinary research projects that provided the GPS data for the present study.

References

- Agatza - Balodimou A.M., Mitsakaki C., Papazissi K., Veis G., (1994) Tectonic deformation in the Corinthian Gulf from geodetic data (in Greek). *Τεχνικά Χρονικά Α, Τομ. 14, Τεύχ. 3*.
- Anastasiou D., Paradissis D., Ganas A., Marinou A., Papazissi K., Drakatos G., Makropoulos K. (2009) Crustal Deformation from GPS measurements at the Ionian Sea: Preliminary Results, *International Technical Laser Workshop on SLR Tracking of GNSS Constellations, Metsovo, Greece, 14-19 September*.
- Argus D.F. and Heflin M.B., (1998) Angular velocity of main plates. Pers. Comm..
- Avallone A., Pierre Briole, Amalia Maria Agatza-Balodimou, Harilaos Billiris, Olivier Charade, Christiana Mitsakaki, Alexandre Necessian, Kalliopi Papazissi, Dimitris Paradissis, George Veis, (2004) Analysis of eleven years of deformation measured by GPS in the Corinth Rift Laboratory area, *C. R. Geoscience 336*, pp. 301–311.
- Bernard P., Lyon-Caen H., Briole P., Deschamps A., Boudin F., Makropoulos K., Papadimitriou, P. Lemeille F., Patau G., Billiris H., Paradissis D., Papazissi K., Cas-

- tarède H., Charade O., Necessian A., Avallone A., Pacchiani F., Zahradnik J., Sacks, S. Linde A., (2006) Seismicity, deformation and seismic hazard in the western rift of Corinth: New insights from the Corinth Rift Laboratory (CRL). *Tectonophysics* 426, 7–30.
- Briole P., Avallone A., Agatza-Balodimou A.M., Billiris H., Charade O., Lyon-Caen H., Mitsakaki C., Papazissi K., Paradissis D., Veis G., Karamanou A., Marinou A. (2002) A ten year analysis of deformation in the Corinthian Gulf via GPS and SAR Interferometry, *11th General Assembly of the WEGENER Project, June 12-14, Athens, Greece*.
- Doutsos T., and Poulimenos G., (1992) Geometry and kinematics of active faults and their seismotectonic significance in the western Corinth-Patras rift (Greece), *Journal of Structural Geology*, Vol. 14, No. 6, pp. 689 -699.
- Ganas A., Serpelloni E., Drakatos G., Kolligri M., Adamis I., Tsimi Ch., Batsi E. (2009) The Mw 6.4 SW-Achaia (Western Greece) Earthquake of 8 June 2008: Seismological, Field, GPS Observations, and Stress Modeling, *Journal of Earthquake Engineering* 13:8,1101 — 1124.
- Ferentinos G., Brooks M., Doutsos T., (1985) Quaternary tectonics in the Gulf of Patras, western Greece, *Journal of Structural Geology*, Vol. 7, No. 6, pp. 713- 717.
- Hollenstein, C. (2006) GPS deformation field and geodynamic implications for the Hellenic plate boundary region. PhD thesis, no. 16593, Eidgenössische Technische Hochschule ETH Zürich.
- Hollenstein Ch., Müller M.D., Geiger A., Kahle H.-G., (2008) Crustal motion and deformation in Greece from a decade of GPS measurements, 1993–2003.
- Kahle H.-G., Müller M. V., Geiger A., Danuser G., Mueller S., Veis G., Billiris H., Paradissis D., (1995) The strain field in northwestern Greece and the Ionian Islands: results inferred from GPS measurements, *Tectonophysics* 249, pp. 41-52.
- Müller M.V., (1995) Satellite geodesy and geodynamics: Current deformation along the West Hellenic Arc. PhD thesis, Eidgenössische Technische Hochschule ETH Zürich. Mitteilungen Nr. 57, Institut für Geodäsie und Photogrammetrie.
- Παπαζάχος Β. και Παπαζάχου Κ., (2003) Οι σεισμοί της Ελλάδας, Εκδόσεις Ζήτη
- Roumelioti, Z., Benetatos, C., Kiratzi, A., Stavrakakis, G., and Melis, N., (2004). A study of the 2 December 2002 (M5.5) Vartholomio (western Peloponnese, Greece) earthquake and of its largest aftershocks, *Tectonophysics* 387(1–4), 65–79.
- Sachpazi M., Hirn A., Clement C., Haslinger F., Laigle M., Kissling E., Charvis P., Hello, Y. Lèpine J.-C., Sapin M., Ansgorge J., (2000) Western Hellenic subduction and Cephalonia Transform: local earthquakes and plate transport and strain, *Tectonophysics* 319, pp. 301–319.
- Veis G., Billiris H., Nakos B., Paradissis D., (1992) Tectonic strain in Greece from Geodetic measurements, *Annales of the Academy of Athens, Vol 67, p.129-166, Greece*.
- http://itrf.ensg.ign.fr/trans_para.php